PHILOSOPHICAL TRANSACTIONS OF THE ROYAL SOCIETY A MATHEMATICAL, PHYSICAL & ENGINEERING SCIENCES

Determination of the Rate Coefficients of A+X $\rightleftarrows $A^{+}+X^{-} and AX+M $\rightleftarrows $A^{+}+X^{-}+M where A is a Metal Atom, X a Halogen Atom and M a Flame Species

N. A. Burdett and A. N. Hayhurst

Phil. Trans. R. Soc. Lond. A 1979 **290**, 299-325
doi: 10.1098/rsta.1979.0001

DETERMINATION OF THE RATE COEFFICIENTS OF $A+X \rightleftarrows A^+ + X^-$ AND $AX+M \rightleftarrows A^+ + X^- + M$ WHERE A IS A METAL ATOM, X A HALOGEN ATOM AND M A FLAME SPECIES

By N. A. BURDETT† and A. N. HAYHURST

Department of Chemical Engineering and Fuel Technology, Sheffield University, Mappin Street, Sheffield

(*Communicated by T. M. Sugden, F.R.S. – Received 25 April 1978*)

CONTENTS

Premixed laminar flat flames of H_2, O_2 and N_2 have been burnt, with trace amounts of various metals (Li, Na, K, Rb, Cs, Ga, In and Tl) and the halogens Cl, Br or I added. Mass spectrometric measurements were made of ion concentrations and also their

† Current address: C.E.G.B., Marchwood Engineering Laboratories, Marchwood, Southampton SO4 4ZB.

variation with time in each flame. These observations establish that a halogen X can cause a metal A to produce ions homogeneously in a flame through the forward steps of

$$A + X \rightleftarrows A^+ + X^- \quad \text{(II)}$$

$$AX + M \rightleftarrows A^+ + X^- + M, \quad \text{(III)}$$

where M is any molecule. The reverse processes are found to facilitate ion recombination. We have measured the rate constants k_2 and k_3 of the ion-producing steps in (II) and (III) over the temperature range 1820–2590 K; they vary with temperature according to $k_2 = A_2 \exp(-\Delta E_2/RT)$ and $k_3 = A_3 T^{-3.5} \exp(-\Delta E_3/RT)$. The activation energies of each reaction were found to equal the appropriate endothermicity, in contrast with previous shock tube determinations of k_3.

For Ga and In with all three halogens, ion recombination rates were measured directly with a little (< 1 vol. %) C_2H_2 also added to the burner supplies. These observations unambiguously gave k_{-2}, the coefficient for recombination in (II), because k_{-3} is very small for these two metals. Also, it was found that these k_{-2} for Ga and In did not equal the ratio of the measured forward rate constant, k_2, and the equilibrium constant for (II). The origin of this departure from detailed balancing is apparently that the ionizing step in (II) proceeds from A and X in their ground states, but the reverse recombination of ions is to ground state Ga, In or Tl and electronically excited ($^2P_{\frac{1}{2}}$) atoms of X. This conclusion was confirmed by computations of k_{-2} using Landau–Zener curve-crossing theory for the products being either ground state atoms or with X excited. The alkali metals K, Rb and Cs, on the other hand, participate in each direction in (II) with A and X only in their ground states (so that detailed balancing does hold), except that there are one or two cases where excited states of A are important and result in anomalously large k_2 and k_{-2}. Li and Na are in an intermediate position, in that ionization in (II) proceeds only from ground state A and X, but both excited and ground state halogen atoms can be the products of ion recombination. Detailed balancing does not strictly hold with Li and Na in (II), but use of it is not likely to generate errors greater than a factor of 2. We were not able to detect any systematic or significant temperature dependence of k_{-2} for any A and X, and conclude that curve-crossing theory gives a good general account of how k_{-2} varies amongst the various A and X.

Detailed balancing always appears to hold for reaction (III) and our values of the three-body ion recombination coefficient, k_{-3}, derived indirectly from k_3 and the equilibrium constant, indicate that it varies as T^{-3}. Also, its magnitude is almost three times larger than predicted by Bates and Flannery's theory, except for a few A and X, where curve-crossing considerations make k_{-3} undetectably small.

1. Introduction

The use of flames as a medium in which to study the gas-phase reactions of ions is now almost common. One example is the ionization of metal atoms, A, in

$$A + M \rightleftarrows A^+ + e^- + M, \quad \text{(I)}$$

where M is some collision partner. The rate coefficients for the ionizing step and reverse recombination process have been measured in flames, principally by Sugden and co-workers, and their work has been evaluated by Ashton & Hayhurst (1973). When, however, alkali metal atoms are present in a flame together with halogen atoms X, new routes for the production and recombination of ions in

$$A + X \rightleftarrows A^+ + X^- \quad \text{(II)}$$

are opened up (Padley *et al.* 1961; Hayhurst & Sugden 1967). In addition, we consider below for the first time the possibility that ions can be generated and consumed in

$$AX + M \rightleftarrows A^+ + X^- + M. \quad \text{(III)}$$

Such reactions occur in shock tubes (Berry *et al.* 1968; Hartig *et al.* 1968; Mandl 1971; Ewing *et al.* 1971; Luther *et al.* 1972; Milstein 1973) and can be thought of in terms of an excited AX molecule dissociating into ions rather than atoms. The likelihood of this is governed, *inter alia*, by the relative dispositions of the potential energy curves for AX and its electronically excited states dissociating into either ionic or atomic products. Similar considerations, of course, affect (II). Since the most important potential energy curves in this system are few in number and can generally be described with fair accuracy, there is the possibility that any measured rate constant for (II) or (III) can be compared with theoretical predictions. In addition to their theoretical interest, both reactions are important in practical systems, such as the direct generation of electric power by M.H.D. (Hayhurst & Sugden 1963) and in characterizing the electrical properties of rocket exhausts, where a lack of knowledge of the rate coefficients of all the processes in (II) and (III) has caused difficulty in modelling work (Jensen & Pergament 1971).

2. Experimental

Since the experimental procedures have been described before (Hayhurst *et al.* 1971; Hayhurst & Telford 1977; Burdett & Hayhurst 1977*a*) only the most pertinent details are highlighted here. All the flames were premixed laminar ones of hydrogen and oxygen diluted with nitrogen or occasionally argon. Some details of the most commonly used are given in table 1. They were burnt at atmospheric pressure and had reaction zones, which were almost flat, followed by a burnt gas region some 0.1–0.2 m in length. Each flame was wide enough for conditions on the axis to be well shielded from the surrounding atmosphere for the first 25–30 mm of the burnt gases. Axial temperatures were measured by the sodium D-line technique (Gaydon & Wolfhard 1970). In general, they rose by some 80 K over the first 5 or so millimetres to the steady values given in table 1. In addition, absolute concentrations of free hydrogen atoms were measured with the $SrOH^+/Sr^+$ technique (Hayhurst & Kittelson 1974). This is straightforward to calibrate with the hottest (>2300 K) flames, where [H] actually attains its equilibrium value in the burnt gases, but in cooler ones [H] was arrived at by matching the observed disappearance rate of atomic hydrogen with those predicted from the well characterized overall rate constants (Jensen & Jones 1974) for $H+H+M \longrightarrow H_2+M$ and $H+OH+M \longrightarrow H_2O+M$. In the cooler flames [H] fell from its maximum in the reaction zone by up to a factor of 50 to its value 30 mm downstream, whereas in the hottest flame the corresponding drop in [H] was fourfold. Since these flames are good approximations to one-dimensional flow systems, rates of chemical reactions can be determined by measuring concentrations along the burnt gases, with a distance of 1 mm corresponding to 0.05–0.1 ms. In addition, these flames are possibly unique in being free from the complicating effects of solid surfaces.

The alkali metals Li, Na, K, Rb and Cs were added to a flame in minute quantities by atomizing into the burner supplies an aqueous solution of the particular chloride. The group III*b* metals Ga, In and Tl were also used as additives, with solutions of their nitrates being atomized. Both these and the alkali metals are known (Padley & Sugden 1958; Bulewicz & Sugden 1958; Kelly & Padley 1971) to end up in the reaction zone of a halogen-free flame as either free atoms or molecules of the hydroxide AOH, with the sum of their mole fractions being typically 10^{-8}. The halogens were added from cylinders of the diluent containing known amounts of Cl_2, HBr or HI. In this way it was possible to vary the overall mole fraction of all halogen species from 2×10^{-4} to 8×10^{-3}, without the deliberate addition of any hydrocarbon. This

kept to a minimum the concentrations of those ions, such as H_3O^+, which primarily result from the presence of hydrocarbons (Green & Sugden 1963) and thereby avoided reactions like

$$A + H_3O^+ \longrightarrow A^+ + H_2O + H \qquad (IV)$$

(Hayhurst & Telford 1970) complicating the production of metal ions. As discussed below, these halogens exist in the burnt gases primarily as free atoms X or molecules of HX, with the concentrations of negative ions X^- and salt molecules AX being negligible by comparison, because of the very much smaller amounts of metal present.

TABLE 1. DESCRIPTION OF FLAMES STUDIED

		unburnt gas mole ratios		
No.	temp./K	H_2	O_2	N_2
1	2590	2.98	1.00	1.97
2	2400	2.74	1.00	2.95
3	2080	3.18	1.00	4.07
4	1980	3.09	1.00	4.74
5	1820	3.12	1.00	5.77

Concentrations of both positive and negative ions along the axis of a flame were measured by direct sampling into a quadrupole mass spectrometer. Calibration procedures are available to arrive at absolute ion concentrations (Hayhurst & Telford 1977). The major difficulty with these measurements arises from ions reacting as the sample cools whilst it enters the first vacuum chamber of the spectrometer. The sampling time is in the range 0.1–1.5 μs (Hayhurst & Kittelson 1977), so that only the fastest reactions with relaxation times less than 5 μs alter a mass spectrum. As a matter of procedure, it is essential to check if an observation is subject to sampling perturbations; this is the case if varying the sampling hole diameter affects the observation in question. The negative ions Cl^-, Br^- and I^- have been shown (Burdett & Hayhurst 1977*a*) to react during sampling (in fact, they associatively detach electrons in (V) below) and it is for this reason that most measurements were of $[A^+]$, which are not falsified by sampling effects.

3. BACKGROUND DESCRIPTION

With only a metal added to one of these flames, the level of ionization is initially zero and grows towards a final value described by (I) at equilibrium (Kelly & Padley 1972; Hayhurst & Telford 1972). The major charged species are free electrons and atomic ions A^+. When a halogen is also present, however, negative ions are formed (Burdett & Hayhurst 1977*a*, *b*) in a rapid balance of

$$H + X^- = HX + e^- \qquad (V)$$

and the halogen is largely distributed as either free atoms or molecules of HX, whose concentrations are coupled by

$$H + HX = X + H_2 \qquad (VI)$$

being equilibrated (Phillips & Sugden 1960). The gradual addition of a halogen to an alkali-laden flame can, in certain circumstances, cause the electron concentrations to rise to a maximum and subsequently fall (Padley *et al.* 1961; Hayhurst & Sugden 1967). The increase in $[e^-]$ establishes that reaction (II) becomes more important when halogen is added, because the sum

of equilibria (II), (V) and (VI) is $A+2H = A^+ + e^- + H_2$. Such a scheme leads to higher final $[e^-]$ than (I), whenever [H] exceeds its value for local equilibrium, which is often the case (Jenkins & Sugden 1969). The falling electron densities at higher halogen concentrations can be caused by negative ion formation via the reverse of (V), as well as metal atoms being removed to form the salt AX (Bulewicz *et al.* 1961) in

$$A + HX = AX + H. \qquad \text{(VII)}$$

At this stage it should be noted that if (III) operates to the exclusion of (II), addition of schemes (III), (V) and (VII) gives (I). Because of this, reaction (III) cannot, as (II) does, lead to a higher equilibrium level of ionization than (I), but probably accelerates the rate of approach to a balance of (I). From this we conclude that reaction (II) must be operating whenever a halogen causes the value of $[e^-]$ corresponding to local balance of (I) to be exceeded. Also, it is clear that scheme (II) is very sensitive to [H], whereas (III) is not.

TABLE 2. COMPUTED VALUES OF ϕ ($=[AOH]/[A]$) AND ψ ($=[AX]/[A]$) 10 mm DOWN FLAME 3 (TEMP. = 2110 K) WITH 0.25 VOL. % OF HALOGEN PRESENT

		ψ		
metal	ϕ	Cl	Br	I
Li	5.5	1342	12	0.37
Na	0.025	0.40	0.51	0.040
K	0.078	1.4	2.0	0.16
Rb	0.14	2.0	3.8	0.48
Cs	0.99	5.2	5.9	0.39
Ga	11	18	22	2.8
In	0.27	1.9	2.4	0.16
Tl	0	0.042	0.074	0.015

From the outset we assume that both (II) and (III) proceed in these systems, in addition to (I). A formal description is completed by stating that these metals form various amounts of their hydroxide (James & Sugden 1955; Bulewicz & Sugden 1958) by a rapid equilibration of

$$A + H_2O = AOH + H. \qquad \text{(VIII)}$$

Reactions (VII) and (VIII) are easily rapid enough for the ratios $\phi = [AOH]/[A]$ and $\psi = [AX]/[A]$ to be calculated from their equilibrium constants, which in turn may be computed by standard statistical mechanical methods. This has been done for bond lengths, vibration frequencies and dissociation energies of H_2O, AOH, HX and AX from a variety of sources (Honig *et al.* 1954; Rice & Klemperer 1957; Klemperer & Rice 1957; Barrett & Mandel 1958; Herzberg 1960, 1966; Bulewicz *et al.* 1961; Jensen & Padley 1966*a*; Gordy & Cook 1970; Kelly & Padley 1971) as well as the J.A.N.A.F. tables (1965). Table 2 gives the calculated ϕ and ψ for every combination of A and X at a point 10 mm (or 0.64 ms) down flame 3, where the temperature is 2110 K and the total halogen content is assumed to be 0.25 vol. %. Clearly hydroxide formation is very important for Li, Cs, In and Ga, but of little consequence for Na, K and Tl. Salt formation is generally of great significance for chlorides and bromides (except with Tl), but not for iodides, except with Ga and possibly also Li, Cs and Rb. The different ψ for chlorides and bromides on the one hand and iodides on the other is due partly to the smaller dissociation

energies of iodides, but also to [HI] being less than [HBr] or [HCl]. In fact, the equilibrium constants of (VI) are such (Burdett & Hayhurst 1977*a*) that chlorine mainly exists in these flames as HCl, iodine almost exclusively as free atoms, and bromine has both forms roughly equally important.

4. Results

In every case the metal gave A^+ as the only positive ion, apart from insignificant quantities of its hydrate. Hydration was most important for Li with $[Li^+]/[Li^+.H_2O]$ being as low as unity in flame 5, whereas with Cs^+ the corresponding ratio in the same flame is at least 500. The amount of hydrate depended on the diameter of the sampling inlet orifice, which establishes that hydration is at least partly associated with sampling. On the occasions when ion hydrates constituted a significant portion of the total number of positive ions, their observed abundances were simply added to that of A^+ to provide a better estimate of $[A^+]$.

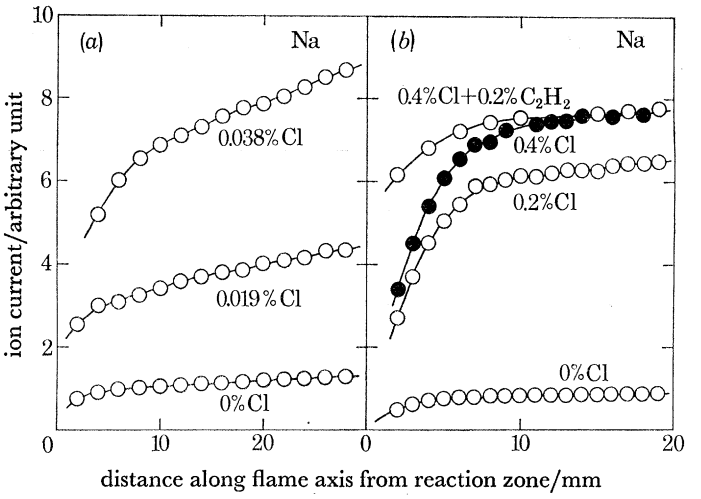

Figure 1. Variation of $[Na^+]$ along a flame axis both with and without chlorine added to: (*a*) flame 5 at 1820 K, (*b*) flame 3 at 2080 K with larger amounts of chlorine and on one occasion also with 0.2 vol. % C_2H_2.

Figure 1 (*a*) gives $[Na^+]$ measured along flame 5 both without any other additive and with two different quantities of chlorine present. It is clear that small amounts of chlorine can cause significant increases in the rate of production of ions, presumably because of processes (II) and (III). It is also worth noting that in none of the cases of figure 1 (*a*) is equilibrium attained. This is not the case for certain concentrations of halogen with Li and Na. In fact, figure 1 (*b*) shows $[Na^+]$ in the hotter flame 3 for much larger additions of chlorine and with 0.4 vol. % of it, a small quantity of C_2H_2 boosts $[Na^+]$ near the reaction zone, but not after 12 mm downstream. The effect of C_2H_2 close to the reaction zone is accounted for by charge exchange in processes like (IV) between metal atoms and ions (e.g. CHO^+, $C_3H_3^+$, H_3O^+, etc.) formed during the combustion of a hydrocarbon (Knewstubb & Sugden 1959; Hayhurst & Kittelson 1978). Otherwise, the indications are that $[Na^+]$ has come close to its equilibrium value 15 mm downstream with 0.4 % of chlorine added, irrespective of whether C_2H_2 is also present or not. Comparison of figures 1 (*a*) and (*b*) shows that small additions of halogen do not necessarily result in equilibrium situations, whereas larger ones can.

Figure 2 shows other cases of equilibrium being approached. Figure 2 (*a*) gives $[Li^+]$ rising

slowly along flame 4 (without halogen present) towards some final value, which can be exceeded on the addition of bromine. The decay of $[Li^+]$ after its maximum is probably due to a lowering of the local equilibrium $[Li^+]$, as [H] decreases, with consequent shifts in equilibria such as (VII) and (VIII). It is however clear from figure 2 (*a*) that recombination reactions are in general likely to be most important. In fact, it is only with very small amounts of bromine added, at positions close to the reaction zone, that recombination is relatively insignificant. Figure 2 (*b*) typifies the situation for Rb and Cs, the most rapid of the metals to undergo collisional ionization in (I). Here $[Cs^+]$ comes close to its equilibrium value at 20 mm along flame 4, even when no halogen is present. The addition of chlorine in this case evidently lowers both the rate of production of ions and their ultimate concentration, because of the formation of CsCl.

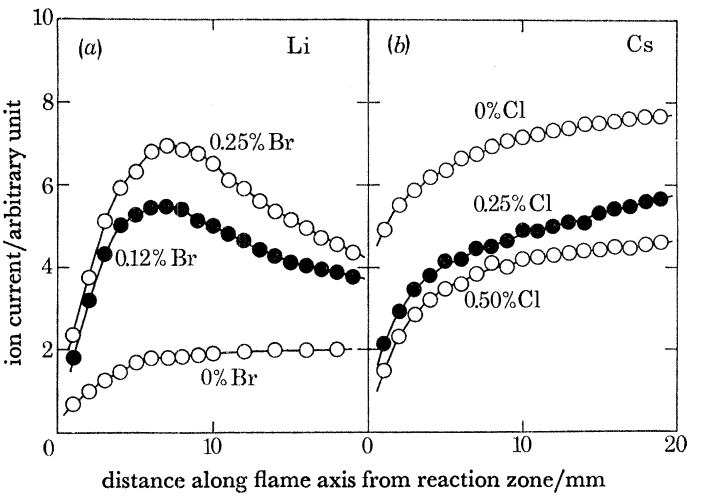

FIGURE 2. Measured positive ion concentrations along flame 4 for: (*a*) Li^+ with and without Br present, (*b*) for Cs and Cl.

5. ANALYSIS

5.1. *Approach to equilibrium from below*

We first examine the consequences of ignoring all recombination reactions, a situation typified by figure 1 (*a*), where $[A^+]$ is nearly always well below its equilibrium value. In the halogen-free flame the rate of ionization is

$$d[A^+]/dt = k_1[A][M], \tag{1}$$

where k_1 is the rate coefficient of the forward step of (I). The overall mass balance on the metal is in general $[A]_T = [A] + [AOH] + [AX] + [A^+] = [A](1 + \phi + \psi) + [A^+]$, where $[A]_T$ is the total concentration of metal in all its forms. Equation (1) thus becomes

$$\frac{d[A^+]_0}{dt} = k_1[M]\left(\frac{[A]_T - [A^+]_0}{1+\phi}\right), \tag{2}$$

where the subscript 0 describes a quantity in the absence of halogen. On adding halogen, the extra ionization processes in (II) and (III) leads to the general rate expression:

$$\frac{d[A^+]}{dt} = \left(\frac{[A]_T - [A^+]}{1+\phi+\psi}\right)(k_1[M] + k_2[X] + k_3[M]\psi).$$

The ratio of the rates of positive ion production with and without halogen now becomes

$$\frac{\mathrm{d}[\mathrm{A}^+]/\mathrm{d}t}{\mathrm{d}[\mathrm{A}^+]_0/\mathrm{d}t} = \left(\frac{[\mathrm{A}]_\mathrm{T}-[\mathrm{A}^+]}{[\mathrm{A}]_\mathrm{T}-[\mathrm{A}^+]_0}\right)\left(\frac{1+\phi}{1+\phi+\psi}\right)\left(1+\frac{k_2[\mathrm{X}]}{k_1[\mathrm{M}]}+\frac{k_3\psi}{k_1}\right). \tag{3}$$

The use in equation (3) of the ionization rate with halogen present relative to that without it eliminates the need for accurate calibration of the atomizer and mass spectrometer. Instead, it is only necessary to know the term

$$Q = \left(\frac{[\mathrm{A}]_\mathrm{T}-[\mathrm{A}^+]}{[\mathrm{A}]_\mathrm{T}-[\mathrm{A}^+]_0}\right),$$

which has been estimated in the following ways:

(i) If the degree of ionization is always small, then $[\mathrm{A}^+]$ and $[\mathrm{A}^+]_0 \ll [\mathrm{A}]_\mathrm{T}$ and Q is unity. This situation can usually be realized for Li, Na, Ga, In and Tl, as well as K at low temperatures.

(ii) When the metal is present in small concentrations, no halogen is added and the condition $K_1 \gg 4[\mathrm{A}]_\mathrm{T}$ holds, where K_1 is the equilibrium constant of (I); it can be shown that ionization is complete at equilibrium, in that $[\mathrm{A}]_\mathrm{T} = [\mathrm{A}^+]_\mathrm{eq}$. This means that $[\mathrm{A}]_\mathrm{T}$ may be measured with the mass spectrometer, using a small amount of acetylene to accelerate ionization, if necessary. In this case Q may be arrived at by substituting the measured ion currents: $[\mathrm{A}^+]_\mathrm{eq}$ $(=[\mathrm{A}]_\mathrm{T})$, $[\mathrm{A}^+]$ and $[\mathrm{A}^+]_0$ into the above expression.

(iii) When neither of the above simplifications holds, the rate of production of A^+ in the absence of halogen can be measured. From equation (2), we have

$$[\mathrm{A}]_\mathrm{T} = \frac{\mathrm{d}[\mathrm{A}^+]_0}{\mathrm{d}t}\,\frac{(1+\phi)}{k_1[\mathrm{M}]}+[\mathrm{A}^+]_0,$$

which with known values of k_1 (Kelly & Padley 1972; Ashton & Hayhurst 1973), ϕ and the flame velocity, enables a mean value of $[\mathrm{A}]_\mathrm{T}$ to be deduced from a measured ionization rate. Its units will be those of ion current. Fairly reproducible values of $[\mathrm{A}]_\mathrm{T}$ and hence Q may be derived this way, but the extra complications mean that this method was avoided, whenever possible.

Knowing Q, we can transform equation (3) to

$$\frac{\mathrm{d}[\mathrm{A}^+]/\mathrm{d}t}{\mathrm{d}[\mathrm{A}^+]_0/\mathrm{d}t}\left(\frac{1+\phi+\psi}{Q(1+\phi)}\right) = 1+\frac{k_2[\mathrm{X}]}{k_1[\mathrm{M}]}+\frac{k_3K_7K_9[\mathrm{X}]}{k_1K_6\gamma^2}, \tag{4}$$

where γ is the ratio of the local hydrogen atom concentration to its equilibrium value, i.e. $[\mathrm{H}]/[\mathrm{H}]_\mathrm{eq}$, and K_9 is the equilibrium constant of

$$\mathrm{H}+\mathrm{H} = \mathrm{H}_2. \tag{IX}$$

Writing now the left hand side of equation (4) as R, we obtain

$$\frac{k_1(R-1)\,[\mathrm{M}]}{[\mathrm{X}]} = k_2+\frac{k_3K_7K_9[\mathrm{M}]}{K_6}\,\frac{1}{\gamma^2}. \tag{5}$$

R corresponds to the ratio of the effective ionization rates with and without halogen present, and the left-hand side of equation (5) is proportional to the effective increase in the rate of ionization per metal atom and per halogen atom. The right hand side of equation (5) indicates that the two additional ionization steps in (II) and (III) are only distinguishable because the first term, k_2, is independent of γ, in contrast to the second, which depends on k_3/γ^2. Clearly then, any experimental separation of the contributions from (II) and (III) will be easiest when $\gamma \gg 1$, i.e. in cool fuel-rich H_2 flames.

5.2. *Near equilibrium situations*

If now a steady state is assumed for $[A^+]$, this can be shown to be characterized by

$$\frac{[A^+]^2}{[A^+]_0^2} = \frac{Q}{K_1}\left(\frac{1+\phi}{1+\phi+\psi}\right)\left(\frac{k_1[M]+k_2[X]+k_3[M]\,\psi}{k_{-1}(1-\lambda)[M]+k_{-2}\lambda+k_{-3}[M]\,\lambda}\right), \tag{6}$$

where $\lambda = [X^-]/([X^-]+[e^-]) = [X^-]/[A^+]$ and is governed entirely by an equilibration of (V). In addition, the rate coefficient for the backward step in (I) is denoted by k_{-1} etc. Solutions of this equation were only attempted for the real situation of Q being effectively unity, which precludes the metals Rb and Cs. Consider then $Q = 1$ and put

$$\epsilon = \left(\frac{1+\phi}{1+\phi+\psi}\right)\frac{[A^+]_0^2}{K_1[A^+]^2};$$

equation (6) becomes

$$\begin{aligned} 0 &= k_1[M]\{\epsilon-(1-\lambda)/K_1\}+k_2(\epsilon[X]-\lambda/K_2)+k_3[M]\,(\epsilon\psi-\lambda/K_3) \\ &= \alpha_1 k_1+\alpha_2 k_2+\alpha_3 k_3. \end{aligned} \tag{7}$$

Derivation of the coefficients α_1, α_2 and α_3 (defined by a comparison of the above pair of equations) from the experimentally observed ion concentrations in principle enables k_2 and k_3 to be arrived at in terms of k_1. It might be noted that equation (7) assumes that $K_2 = k_2/k_{-2}$, $K_3 = k_3/k_{-3}$, etc. It will be seen below that this might not always be true, so that this approach is not universally applicable.

5.3. *Approach to equilibrium from above*

In this case only recombination reactions are assumed to operate and

$$-\frac{1}{[A^+]^2}\frac{d[A^+]}{dt} = k_{-1}[M]\,(1-\lambda)+\lambda(k_{-2}+k_{-3}[M]). \tag{8}$$

It is clear that the recombination steps in (II) and (III) are indistinguishable and only a composite recombination coefficient $k_r = k_{-2}+k_{-3}[M]$ can be determined. The measurement of k_r can consequently be achieved in the same way as for H_3O^+ and NO^+ recombining with the halide ions in flames (Burdett & Hayhurst 1976, 1978).

6. Determination of rate constants

6.1. *For approach to equilibrium from below*

We shall first discuss the determination of rate constants when the degree of ionization is small and no hydrocarbon is present in the flame. Equation (5) suggests that k_2 and k_3 are the intercept and slope of plots of $k_1(R-1)[M]/[X]$ against $K_7K_9[M]/K_6\gamma^2$. To present the measured $[A^+]$ in this form, they were first numerically smoothed and then differentiated (Hershey *et al.* 1967) with respect to distance along the flame axis. In addition, the slight variations in temperature were taken into account, when computing equilibrium constants, etc; values of k_1 were taken from Ashton & Hayhurst (1973) for the alkali metals and from Kelly & Padley (1969) for the group IIIb metals. Figure 3 shows some observations for potassium and three bromine concentrations in flame 5, plotted as $\delta = 1$. It is clear that a curve, rather than a straight line, is obtained. The curvature is believed to originate in the large temperature dependence of k_3,

which is expected (Mandl 1971) to vary as $T^{-\frac{7}{2}}\exp(-\Delta H_3/RT)$, where ΔH_3 is the fairly large endothermicity of reaction (III). To demonstrate that this may well account for the curvature, $k_1(R-1)[\mathrm{M}]/[\mathrm{X}]$ is also plotted in figure 3 against $\delta K_7 K_9[\mathrm{M}]/K_6\gamma^2$, where δ is a correction factor equal to $(T_\mathrm{f}/T)^{\frac{7}{2}}\exp\{-(\Delta H_3/R)(T^{-1}-T_\mathrm{f}^{-1})\}$, T being a local temperature and T_f an average one for the flame. The original data now give a good fit to a straight line.

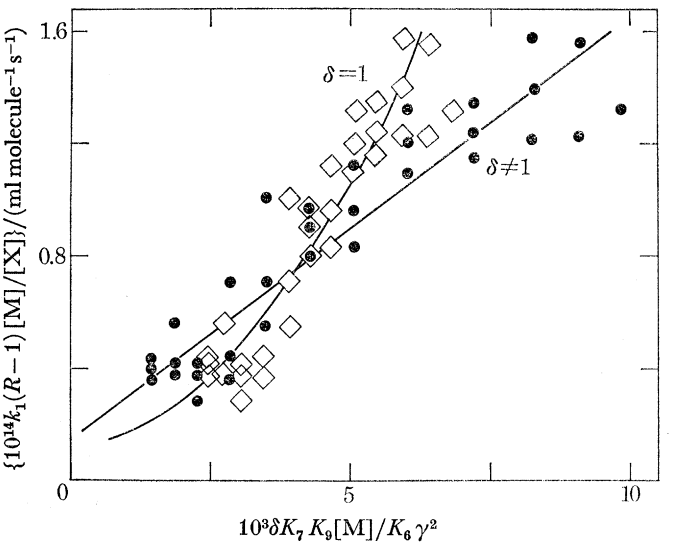

FIGURE 3. Experimental plots of $k_1(R-1)[\mathrm{M}]/[\mathrm{X}]$ against $\delta K_7 K_9[M]/K_6\gamma^2$ for potassium and three different amounts of bromine in flame 5. The raw data (◇) are presented as $\delta = 1$ and re-plotted as $\delta \neq 1$ (●) to cater for T and k_3 varying along the flame.

This procedure has been applied to as many flames and combinations of metal and halogen as possible. It was occasionally found convenient to plot the results against $Z = K_7 K_9[\mathrm{M}]\exp(-\Delta H_3/RT)/T^{\frac{7}{2}}K_6\gamma^2$ as abscissa. The slope of the best fit then becomes the pre-exponential factor A_3 in the expression $k_3 = A_3 T^{-3.5}\exp(-\Delta H_3/RT)$, which will be shown below to hold quite well. Also, this approach assumes k_2 is much less sensitive to temperature than k_3, which is possibly not strictly true, but will be seen below to be a reasonable approximation.

Figure 3 indicates that in this case the contribution to the overall ionization rate from reaction (II) is significantly less than that from (III) at all points beyond a few millimetres downstream in this flame. This means that this approach produces fairly accurate k_3, but occasionally the error in k_2 may be relatively large. In some cases (e.g. with Cs and mostly with Rb) the intercept on the vertical axis is effectively zero and only an upper limit for k_2 can be deduced from the errors in constructing the straight line plot. Such a situation is shown in figure 4 (*a*) for Cs and Br. The opposite behaviour, of the slope (or k_3) being close to zero, is depicted in figure 4 (*b*) for In and Br. Here the region of an almost constant contribution from reaction (II) extends for over 25 mm from the reaction zone, indicating the slowness with which equilibrium is attained. In some instances (e.g. Br with Li or Na) this constancy is limited by the eventual attainment of equilibrium, resulting in a final fall in $(R-1)\,k_1[\mathrm{M}]/[\mathrm{X}]$. This is exemplified by figures 1 (*b*) and 2, where recombination reactions become important after a short distance downstream.

Some experiments were performed using potassium and chlorine in 12 flames all at 1900 K (not shown in table 1), but differing in that half had argon as diluent and half nitrogen. The ratio $[\mathrm{H_2}]/[\mathrm{O_2}]$ in the unburnt gas varied from 5.0 to 2.5, which resulted in the hydrogen

atom disequilibrium parameter γ, covering quite different ranges in each flame. The most fuel-rich had largest γ (Jenkins & Sugden 1969), which resulted in $\phi = [KOH]/[K]$ and $\psi = [KCl]/[K]$ acquiring their minimum values. In addition, reaction (VI) shifts to give maximum $[Cl]/([HCl]+[Cl])$ for the greatest γ. This meant that the increase in ionization rate was observed to be biggest in the most fuel-rich of these flames. The effect of changing the diluent from N_2 to Ar primarily alters the third body M and its efficiency for ionization in (III). Although in principle it should be possible to extract individual ionization efficiencies for H_2, H_2O, N_2 and Ar from these observations, the errors in ϕ, ψ, [H], etc. preclude this. Instead, it was assumed that all argon-containing flames possessed one unique k_3 and those with N_2 had another. This procedure, outlined previously (Burdett & Hayhurst 1977*b*), indicates that $k_3 = 1.5 \times 10^{-18}$ ml molecule^{-1} s^{-1} with N_2 and 8.8×10^{-19} for Ar as M.

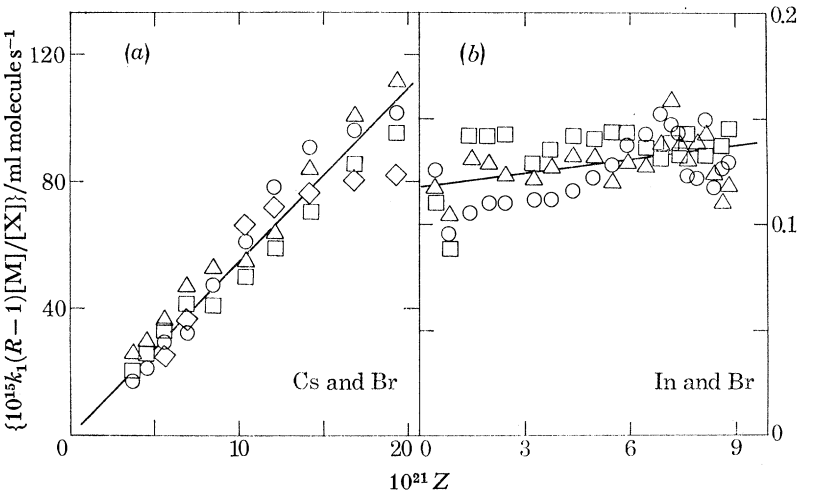

FIGURE 4. Plots of $k_1(R-1)[M]/[X]$ against Z for (*a*) Cs and Br in flame 5 with: 0.097 % Br ○; 0.15 % Br □; 0.19 % Br ◇; 0.24 % Br △; (*b*) In and Br in flame 2 with: 0.097 % Br △; 0.15 % Br ○; 0.19 % Br □.

All 12 flames yielded the same k_2 of 7.2×10^{-14} ml molecule^{-1} s^{-1}. This dependence of process (III) on the nature of the third body, when coupled with (II) remaining unaffected by a change of M, provides strong confirmation that both reactions are producing ions in these flames, in addition to (I). All the values derived for k_2 and k_3 are presented and discussed below. It should, however, be stressed that none of them were found to depend on the diameter of the sampling orifice or on whether the sampling cone was made of chromium or nickel. This establishes the validity of the measurements and their freedom from sampling effects.

6.2. *With steady state* $[A^+]$

We now describe some of the studies made when $[A^+]$ was effectively at its equilibrium value. Figure 5 shows variations of measured $[Na^+]$ and the $[e^-]$ calculated from them using K_5, when chlorine was added to a sodium-containing flame. The concentration of Na^+ was kept at its equilibrium value by adding acetylene, sufficient to provide an ionization boost, but not enough to produce super-equilibrium $[Na^+]$ or large amounts of H_3O^+. It is interesting that $[e^-]$ at 3 mm displays a maximum; indeed $[e^-]$ at this distance is always greater than without any halogen added. At larger distances downstream, the lower [H] lead to monotonically decreasing $[e^-]$.

These results are identical with those of earlier investigators (Hayhurst & Sugden 1967), who measured [e$^-$] with a microwave cavity. The maximum [e$^-$] in figure 5 is clear evidence that process (II) is operating. This does not mean that reaction (III) does not contribute at all, but that at 3 mm the [H] overshoot is sufficiently large for (II) to dominate the production of charged species.

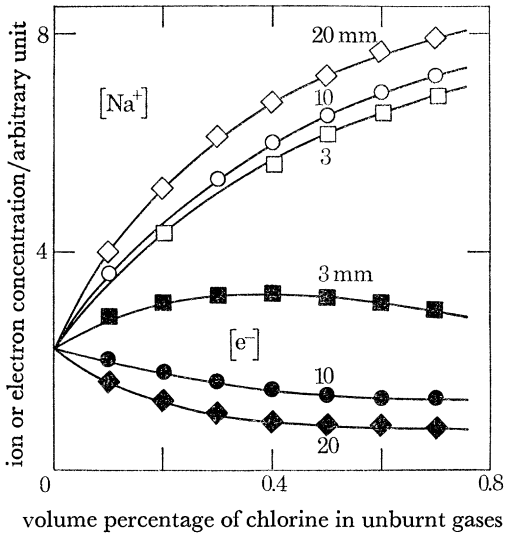

FIGURE 5

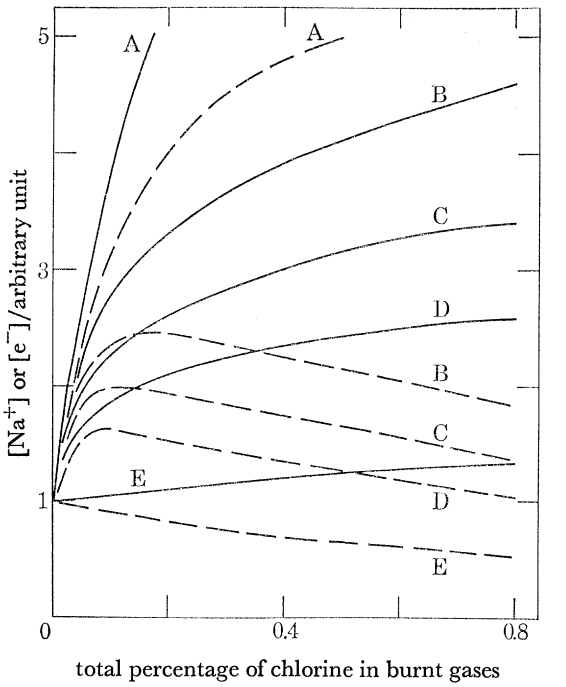

FIGURE 6

FIGURE 5. Measured [Na$^+$] at three different points along flame 3 (2080 K) with various amounts of chlorine added to the burner supplies. Also presented are the [e$^-$] computed from the measured [Na$^+$].

FIGURE 6. Calculated [Na$^+$] (solid lines) and [e$^-$] (broken lines) for various k_2 and k_3 at 3 mm along the burnt gases of flame 3, as in figure 5. Curves A, B, C and D are all for $k_2 = 2 \times 10^{-15}$ ml atom^{-1} s^{-1} and for k_3 equal to 0, 5×10^{-19}, 1×10^{-18} and 2×10^{-18} ml molecule^{-1} s^{-1}, respectively. Curves E are for $k_2 = 0$ and a wide range of k_3.

If no ions are produced in (II), ion concentrations must change with added halogen as a result of the reduction in [e$^-$] and [A], because of negative ions, X$^-$, and salt, AX, being formed. In fact, with (II) inoperative and (I) at equilibrium the size of k_3 is irrelevant, in that it does not affect ion concentrations. As a result, equilibrium ion levels can only be used to derive rate constants if (II) is of sufficient importance for there to be a significant increase in [A$^+$] above the level given by $k_2 = 0$. This means that the use of equation (7) is limited.

It is of interest to consider the effect of scheme (III) on the maximum in [e$^-$]. Figure 6 shows [Na$^+$] and [e$^-$] (solid and broken lines, respectively) calculated from equation (6) and plotted against the total chlorine concentration for different combinations of k_2 and k_3. The conditions are those in figure 5 at 3 mm from the reaction zone. Curve E in figure 6 shows that if $k_2 = 0$, irrespective of the magnitude of k_3, the increase in [Na$^+$] with chlorine added is small and the electron concentration always decreases. The other plots are for one k_2 and increasing k_3. Clearly the larger k_3 becomes, the smaller are ion concentrations. In addition, the maximum in [e$^-$] diminishes and occurs at smaller chlorine concentrations. The shapes of these curves are broadly similar to the experimental ones in figure 5, although the lower slope for small chlorine additions

may possibly be due to a lack of equilibrium. The data at 3 mm in figure 5 have been used to derive α_1, α_2 and α_3 in equation (7) and the resulting $-k_1\alpha_1/\alpha_2$ are plotted against α_3/α_2 in figure 7 (*a*). The straight line there indicates values for k_2 and k_3 of 2.2×10^{-15} and

$$4.4 \times 10^{-19}\,\text{ml molecule}^{-1}\,\text{s}^{-1},$$

respectively, which are roughly $\frac{1}{4}$ and 4 times those derived in § 6.1. Comparison of figures 5 and 6 indicates that this pair of rate constants gives fairly good agreement between experimental and calculated ion and electron profiles.

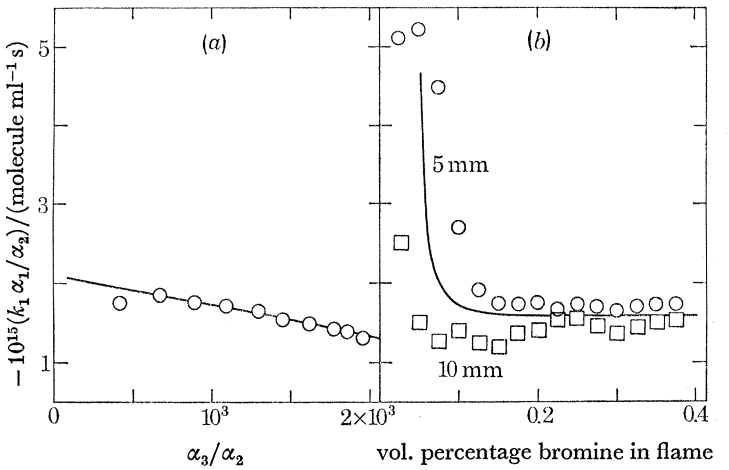

FIGURE 7. Plots of $-k_1\alpha_1/\alpha_2$ against: (*a*) α_3/α_2, for the data in figure 5 for 3 mm along flame 3 with Na and Cl present, (*b*) $[\text{Br}]_\text{T}$, the sum of the concentrations of all bromine-containing species at two distances from the reaction zone of flame 3.

In general, this method does not yield very reproducible or accurate results, since small errors in [H], [A^+], [halogen], etc. can produce large errors in the derived rate coefficients. The method works best when $k_3 \simeq 0$, as in figure 4 (*b*), and equation (7) gives $k_2 = -k_1\alpha_1/\alpha_2$. If therefore α_1/α_2 is found to be constant over a range of halogen and H atom concentrations, it is reasonable to put $k_3 \simeq 0$. Figure 7 (*b*) shows a plot of $-k_1\alpha_1/\alpha_2$ against $[\text{Br}]_\text{T}$ in a sodium-laden flame. The constancy of $-\alpha_1/\alpha_2$ over a range of $[\text{Br}]_\text{T}$ is good evidence for the correctness of this approach. The high values at small $[\text{Br}]_\text{T}$ indicate a lack of attainment of equilibrium, which is more pronounced at 5 than 10 mm from the reaction zone. Otherwise, a value of

$$k_2 = -k_1\alpha_1/\alpha_2 = 1.6 \times 10^{-15}\,\text{ml molecule}^{-1}\,\text{s}^{-1}$$

is indicated, which compares well with $1.0 \times 10^{-15}\,\text{ml molecule}^{-1}\,\text{s}^{-1}$ from the approach outlined above in § 6.1. In fact, this method gives 'good' values of k_2, whenever $k_3 \simeq 0$, these usually being slightly higher than those measured from rates of ionization. Also, this approach did not work well for Ga, In or Tl, since the addition of acetylene tended to produce super-equilibrium ion concentrations and large $[H_3O^+]$, even in the absence of halogen. The method was not used to measure k_2 and k_3 together, except with Na and Cl, but was employed to indicate a large k_2. The metals producing significant electron concentration increases were Li, Na and K (although, with Cl, only close to the reaction zones of cooler flames) with all the halogens, and Rb only with I.

These studies of equilibrium ion levels refer to one sampling point with varying amounts of halogen. It is simple to extend the analysis to cover examples, such as Li and Br in figure 2 (*a*), where equilibrium is attained after a short time. Clearly at the maximum in $[Li^+]$, the rates of production and recombination of Li^+ are equal. This steady state probably continues downstream (because the 'overshoot' is only by a factor of three or less), with $[Li^+]$ falling as equilibria shift owing to diminution of [H]. If this is so, then equation (6) can be simplified to

$$\left(\frac{[Li^+]}{[Li^+]_0}\right)^2 = \left(\frac{1+\phi}{1+\phi+\psi}\right)\left(\frac{[M]+R'[Br]}{(1-\lambda)[M]+R'\lambda K_1/K_2}\right) \tag{9}$$

since $Q = 1$ and $k_3 \simeq 0$ in this case. R' in equation (9) is k_2/k_1. The solid lines in figure 8 show the right-hand side of this equation as computed along flame 4 with 0.25 % of bromine (i.e. the same conditions as in figure 2 (*a*)) and for R' varying from 0 to 10^5. Also included in figure 8 are the experimental observations from figure 2 (*a*) (as circles) and the match with the computed curves indicates that $R' = 4.9 \times 10^4$. This gives k_2 2.3 times larger than that derived from ionization rates in § 6.1. The agreement is not perfect, but is sufficient to verify the assumption that equilibrium prevails after the maximum in $[Li^+]$ and also that scheme (III) is inoperative for this combination of A and X.

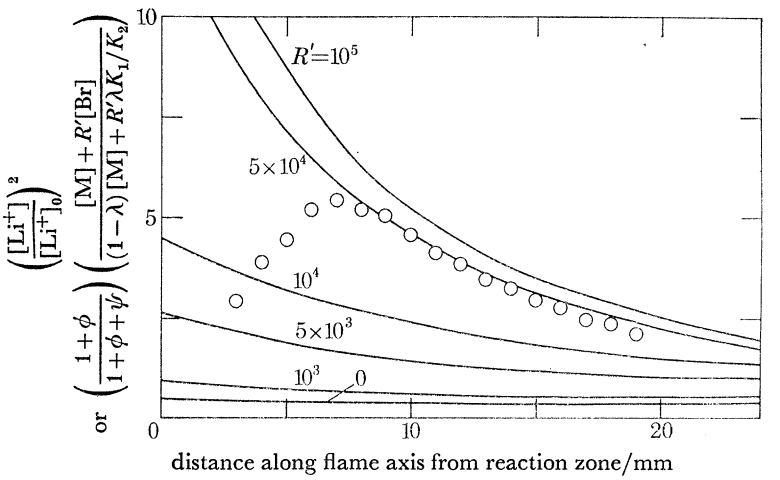

FIGURE 8. The right-hand side of equation (9) (solid lines) as computed for conditions along flame 4 with 0.25 vol.% of bromine added and various guessed values of $R' = k_2/k_1$. The circles give the left-hand side of equation (9), i.e. $([Li^+]/[Li^+]_0)^2$, as derived from the data points for the same conditions in figure 2 (*a*).

6.3. *For super-equilibrium* $[A^+]$

Here the 'overshoot' of ion concentrations above their equilibrium values is large enough for recombination processes to dominate. From equation (8), the ratio of the rates of decay of metal ions with and without halogen present is given by

$$\frac{d[A^+]^{-1}}{dt}\frac{dt}{d[A^+]_0^{-1}} = \frac{k_{-1}[M](1-\lambda)+\lambda(k_{-2}+k_{-3}[M])}{k_{-1}[M]}. \tag{10}$$

Figure 9 shows recombination plots of $1/[A^+]$ against distance (or time) for Ga^+ without added halogen and for 0.4 % bromine present. Under these conditions recombination is entirely in the backward step of (I) in the first case and totally in the reverse of (II) in the second, because $\lambda = 1$ along this flame and $k_{-3}[M] \ll k_{-2}$. Equation (10) then gives the ratio of the slopes of the

two lines in figure 9 to be k_{-2}/k_{-1}. Since k_{-1} can be obtained from the known value (Kelly & Padley 1969) of k_1, through $k_{-1} = k_1/K_1$, k_{-2} may be derived. This straightforward state of affairs was found to apply with Ga and In for all three halogens. With Tl, however, only a composite $k_r = (k_{-2} + k_{-3}[M])$ could be measured, because of the known participation of process (III). The method proved useless for the alkali metals, because of the extra reason that the 'overshoots' of $[A^+]$ above their equilibrium values were too small with 1 % of C_2H_2 in these flames for ionization processes to be ignored.

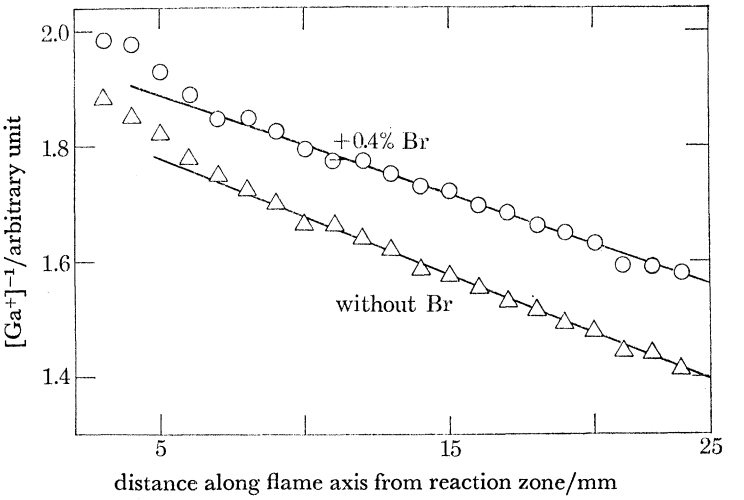

FIGURE 9. Plots of $1/[Ga^+]$ against axial distance along flame 3 without halogen present (△) and with 0.4 % of Br added (○).

7. VALUES OF MEASURED RATE CONSTANTS

7.1. *From ionization rates*

The results are too numerous for all to be presented. It is worth mentioning, however, that they are valid in the sense that they never showed any dependence on the size of the sampling orifice or on whether the sampling nozzle was made of nickel or chromium. The measured k_2 from observing ionization rates are typified by those in figure 10(*a*) plotted logarithmically against $1/T$ for Li, Na and K with all three halogens. Figure 10(*b*) gives the k_{-2} derived from these k_2 and the calculated K_2 for each flame temperature. *Prima facie* these k_{-2} appear to be either independent of temperature or to vary by less than a factor of 2.3 over nearly 800 K. To assess the temperature dependences of k_2 and k_{-2}, information on their associated errors is required. For instance, the k_2 for potassium in flame 2 are all similar to the minimum values measurable and are consequently less accurate than those from lower temperatures. In addition, the small 'overshoots' of [H] near the reaction zones of flames 1 and 2 give greater errors in k_2 for Li and Na with Cl. This is because (II) and (III) both operate in these cases and a separation of the two requires an appreciable change in γ along a flame. There is no such problem for Li and Na with Br and I, where $k_3 \simeq 0$. The high temperature flames proved unusable for Cs, because the ionization rate in (I) was so rapid that reproducible results were difficult to obtain. These caveats apart, the measurements of k_2 and k_3 from this approach are subject to overall errors of just under a factor of 2.

Given this we conclude that k_{-2}, as derived in this way from k_2, varies with temperature as $T^{1\pm2}$. Certainly, our observations are not sufficiently accurate to check Bates & Boyd's (1956) theoretically predicted $T^{-\frac{1}{2}}$ variation, since this suggests a change of only 20% over the temperature range of 800 K here. If k_{-2} is taken to be independent of T, which is reasonable in view of the measured and theoretical dependences, then K_2 is such that k_2 equals $A_2 \exp(-\Delta E_2/RT)$ and has a constant pre-exponential factor invariant with temperature. The activation energies, ΔE_2, were obtained from Arrhenius plots, as in figure 10(*a*) and are given in table 3. These ΔE_2 are accurate to less than 50 kJ mol^{-1} and are seen to equal the endothermicities, ΔH_2, for reaction (II). On the assumption that this is the case, the pre-exponentials A_2 have been derived and are also listed in table 3. The values quoted there for k_{-2} are averages for the mean temperature of 2200 K; this averaging implies that k_{-2} is not a strong function of temperature. Occasionally, only upper limits can be given for A_2 and k_{-2}. Also, in a few cases there were insufficient measurements of k_2 to both determine the activation energy ΔE_2 and to check that it equals ΔH_2. In such cases ΔE_2 has been taken to equal ΔH_2 in the derivation of A_2.

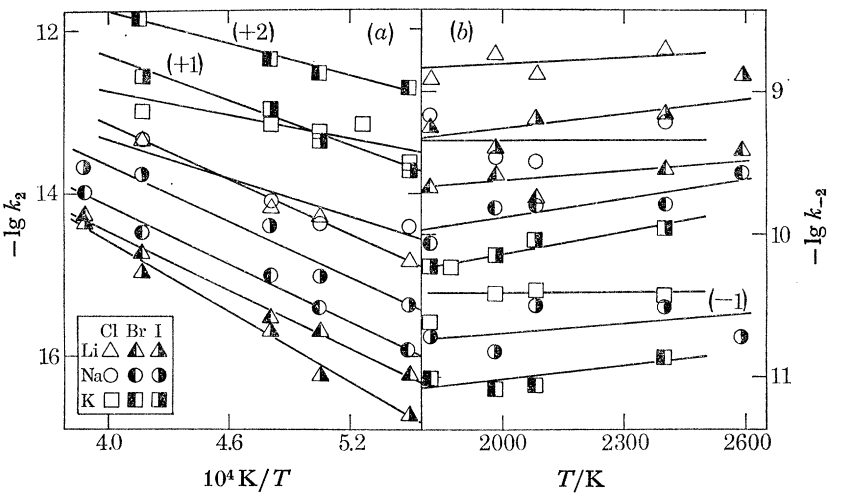

FIGURE 10. (*a*) Arrhenius plots of the measured lg k_2 against $1/T$ for Li, Na and K with all three halogens, (*b*) logarithmic plots of k_{-2}, as derived from k_2 and K_2, against temperature. In one or two combinations of alkali and halogen the points have been shifted vertically, by the amounts shown, for greater clarity.

All the measured k_3 were first converted to corresponding values of k_{-3}, using the appropriate computed equilibrium constant in $k_{-3} = k_3/K_3$. Since ion recombination in the reverse of (III) is strongly exothermic and unlikely to have an activation barrier, k_{-3} was assumed to equal $A_{-3}\,T^{-n}$ and n determined from plots of log k_{-3} against log T. The resulting values of n are listed in table 3 and it is clear that there is quite a spread of values, although their mean is 3.4 ± 1.5. This should be compared with Bates & Flannery's theoretical prediction (1968) of $n = 3$. Again, the accuracy of our observations is not sufficient to decide on n with any great certainty; instead, we shall take $n = 3$, with the experimental evidence for this from table 3 being suggestive, rather than compelling. With $k_{-3} = A_{-3}\,T^{-3}$, the ionization rate constant k_3 is approximately of the form $A_3\,T^{-3.5}\exp(-\Delta H_3/RT)$. This has been checked by plotting the original measurements of k_3 as lg $(k_3\,T^{3.5})$ against $1/T$ and a variety of these is given in figure 11. The data in fact do fit to straight lines, the slopes of which provide values of the activation energy ΔE_3. The derived ΔE_3 are listed in table 3 and have associated errors of around ± 50 kJ mol^{-1}. It is clear that

ΔE_3 and ΔH_3 equal each other within experimental error. Table 3 also includes values of both A_3, deduced on the assumption that $\Delta E_3 = \Delta H_3$, and the corresponding A_{-3}. On the several occasions where the forward step of reaction (III) was not particularly important, upper limits for A_3 and A_{-3} have been estimated.

TABLE 3. MEASURED KINETIC PARAMETERS (for details see text) WITH $k_2 = A_2 \exp(-\Delta H_2/RT)$, $k_3 = A_3\, T^{-3.5} \exp(-\Delta H_3/RT)$ AND $k_{-3} = A_{-3}\, T^{-3}$

(Units are either kJ mol^{-1} or the ml molecule^{-1} s^{-1} system; 1.5 (−10) means 1.5×10^{-10})

A	X	ΔH_2	ΔE_2	A_2	k_{-2}	ΔH_3	ΔE_3	n	A_3	A_{-3}
Li	Cl	171	195	1.5 (−10)	1.6 (−9)	643	646	3.1	2.9 (7)	1.4 (−17)
Li	Br	195	225	2.7 (−11)	2.7 (−10)	614	—	—	<6.0 (2)	<3.5 (−22)
Li	I	224	276	7.1 (−11)	7.1 (−10)	568	—	—	<2.0 (2)	<1.6 (−22)
Na	Cl	147	143	4.9 (−11)	4.8 (−10)	554	570	3.3	3.8 (7)	2.6 (−17)
Na	Br	172	222	1.7 (−11)	1.6 (−10)	533	—	—	<1.2 (3)	<9.9 (−22)
Na	I	200	213	2.7 (−11)	2.3 (−9)	503	—	—	<4.2 (3)	<4.5 (−21)
K	Cl	70	72	3.8 (−12)	4.3 (−11)	494	489	1.5	1.1 (7)	1.1 (−17)
K	Br	95	121	1.1 (−12)	1.0 (−11)	474	453	4.1	8.0 (6)	9.5 (−18)
K	I	123	163	8.2 (−12)	8.4 (−11)	444	474	1.6	7.5 (6)	1.2 (−17)
Rb	Cl	54	—	<1.0 (−13)	<1.0 (−12)	478	532	2.2	6.3 (6)	7.0 (−18)
Rb	Br	78	—	1.1 (−13)	1.5 (−12)	463	464	5.4	6.8 (6)	8.9 (−18)
Rb	I	107	—	1.9 (−12)	1.8 (−11)	442	411	4.7	3.5 (6)	6.2 (−18)
Cs	Cl	26	—	<1.0 (−13)	<1.0 (−12)	465	464	2.7	3.7 (6)	4.6 (−18)
Cs	Br	50	—	<2.5 (−14)	<2.1 (−13)	443	411	3.8	2.7 (6)	4.1 (−18)
Cs	I	79	—	1.2 (−13)	1.5 (−12)	407	454	6.5	1.0 (6)	2.1 (−18)
Ga	Cl	234	232	1.8 (−11)	3.0 (−10)	706	—	—	<8.0 (1)	<3.8 (−23)
Ga	Br	258	279	4.9 (−12)	5.4 (−11)	684	—	—	<2.3 —	<1.3 (−24)
Ga	I	287	287	1.4 (−11)	1.1 (−10)	664	—	—	<1.0 —	<7.5 (−25)
In	Cl	213	218	3.6 (−11)	3.9 (−10)	644	—	—	<2.6 (2)	<1.5 (−22)
In	Br	237	254	3.4 (−11)	3.1 (−10)	621	—	—	<5.1 (1)	<3.5 (−23)
In	I	266	297	2.1 (−11)	2.1 (−10)	588	—	—	<3.7 —	<3.3 (−24)
Tl	Cl	247	222	5.7 (−12)	5.3 (−11)	607	611	2.7	4.5 (6)	2.1 (−18)
Tl	Br	270	317	2.4 (−12)	2.8 (−11)	591	566	3.8	3.1 (6)	2.1 (−18)
Tl	I	299	295	7.2 (−12)	5.6 (−11)	580	584	2.5	2.1 (6)	1.7 (−18)

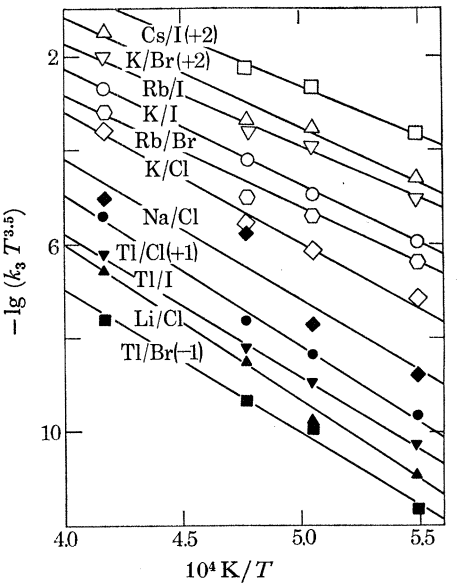

FIGURE 11. Modified Arrhenius plots of lg ($k_3\,T^{3.5}$) against $1/T$ for typical pairs of halogen and metal. Some points have been shifted vertically by the amounts shown for greater clarity.

7.2. *From steady state* [A^+]

This method was only used to provide quantitative results in a limited number of cases. Otherwise, as has already been seen, much evidence emerged from it which confirms the scheme of reactions already adopted. Table 4 lists the measured k_2 for the alkali metals, whenever $k_3 \simeq 0$. Alongside are the k_2 calculated from the A_2 and ΔH_2 in table 3. The values measured here are seen to be usually higher than those indicated by rates of ionization, although there is usually agreement to within a factor of 2, except for Na and I. This is taken to be an indication that, for the reasons discussed above, the rate coefficients from this approach are less accurate than those in table 3.

TABLE 4. VALUES OF k_2 IN ml molecule^{-1} s^{-1} MEASURED UNDER EQUILIBRIUM CONDITIONS AND COMPARED WITH THOSE IONIZATION RATES IN TABLE 3

(6.0 (−16) means 6.0×10^{-16})

		measured k_2			k_2 calculated from table 3		
A	X	flame 3	flame 4	flame 5	flame 3	flame 4	flame 5
Li	Br	6.0 (−16)	5.0 (−16)	2.0 (−16)	3.4 (−16)	1.9 (−16)	6.8 (−16)
Li	I	3.1 (−16)	1.8 (−16)	1.0 (−16)	1.7 (−16)	8.7 (−17)	2.6 (−17)
Na	Br	1.6 (−15)	1.0 (−16)	8.0 (−17)	8.1 (−16)	4.9 (−16)	2.0 (−16)
Na	I	4.3 (−15)	1.0 (−15)	9.1 (−16)	2.6 (−16)	1.4 (−16)	4.9 (−17)

TABLE 5. VALUES OF k_{-2} IN ml ion^{-1} s^{-1} AS MEASURED FROM IONIZATION RATES AND DIRECTLY AND ALSO AS COMPUTED

(v.s. means very small ($< 10^{-20}$).)

A	X	from ionization kinetics	from recombination kinetics	theoretical leading to ground $^2X_{\frac{3}{2}}$	theoretical leading to excited $^2X_{\frac{1}{2}}$	from Hayhurst & Sugden (1967) at 1800 K
Li	Cl	1.6 (−9)	—	1.5 (−9)	3.2 (−9)	—
Li	Br	2.7 (−10)	—	1.6 (−9)	2.5 (−9)	—
Li	I	7.1 (−10)	—	1.5 (−9)	1.0 (−9)	—
Na	Cl	4.8 (−10)	—	5.3 (−10)	5.6 (−10)	6.0 (−10)
Na	Br	1.6 (−10)	—	1.0 (−9)	5.0 (−10)	3.5 (−10)
Na	I	2.3 (−9)	—	7.1 (−10)	3.6 (−11)	4.0 (−10)
K	Cl	4.3 (−11)	—	1.8 (−15)	1.1 (−16)	1.6 (−10)
K	Br	1.0 (−11)	—	1.1 (−12)	v.s.	2.3 (−10)
K	I	8.4 (−11)	—	1.8 (−10)	v.s.	2.5 (−9)
Rb	Cl	< 1.0 (−12)	—	1.2 (−19)	v.s.	—
Rb	Br	1.5 (−12)	—	3.0 (−14)	v.s.	—
Rb	I	1.8 (−11)	—	2.8 (−11)	v.s.	—
Cs	Cl	< 1.0 (−12)	—	v.s.	v.s.	—
Cs	Br	< 2.1 (−13)	—	3.2 (−20)	v.s.	—
Cs	I	1.5 (−12)	—	1.2 (−13)	v.s.	—
Ga	Cl	3.0 (−10)	4.0 (−9)	3.2 (−10)	8.9 (−10)	—
Ga	Br	5.4 (−11)	3.5 (−9)	1.3 (−10)	1.2 (−9)	—
Ga	I	1.1 (−10)	3.3 (−9)	5.9 (−11)	8.1 (−10)	—
In	Cl	3.9 (−10)	1.4 (−9)	4.3 (−10)	1.0 (−9)	—
In	Br	3.1 (−10)	1.9 (−9)	1.8 (−10)	9.1 (−10)	—
In	I	2.1 (−10)	3.5 (−9)	9.1 (−11)	2.2 (−9)	—
Tl	Cl	5.3 (−11)	—	2.3 (−10)	5.6 (−10)	—
Tl	Br	2.8 (−11)	—	6.6 (−11)	5.6 (−10)	—
Tl	I	5.6 (−11)	—	2.8 (−11)	1.9 (−9)	—

PHILOSOPHICAL TRANSACTIONS OF THE ROYAL SOCIETY A MATHEMATICAL, PHYSICAL & ENGINEERING SCIENCES

7.3. *From recombination rates*

Here it only proved possible to measure k_{-2} directly for Ga and In, but with all three halogens. These observed k_{-2} were found not to vary significantly with temperature and their mean values are given in table 5. Also there for comparison are the k_{-2} obtained from the rates of ion production using $k_{-2} = k_2/K_2$. It is noteworthy that the k_{-2} measured directly for Ga and In are significantly larger than from the kinetics of ionization via the equilibrium constant K_2. This difference will be discussed later along with the rest of table 5, after some theoretical computations of k_{-2} have been described.

8. Discussion

8.1. *Introduction*

The similarity between reactions (II) and (III) is brought out by the covalent and ionic potential energy curves for Na and I in figure 12. Given there are the electronic states for the separated atoms Na and I with energies less than that of Na^+ and I^-. In this particular case the combination $Na(3\,^2P)$ and I ($^2P_{\frac{3}{2}}$) is fortuitously close in energy to Na^+ ($^1S_0$) and I^- ($^1S_0$). The

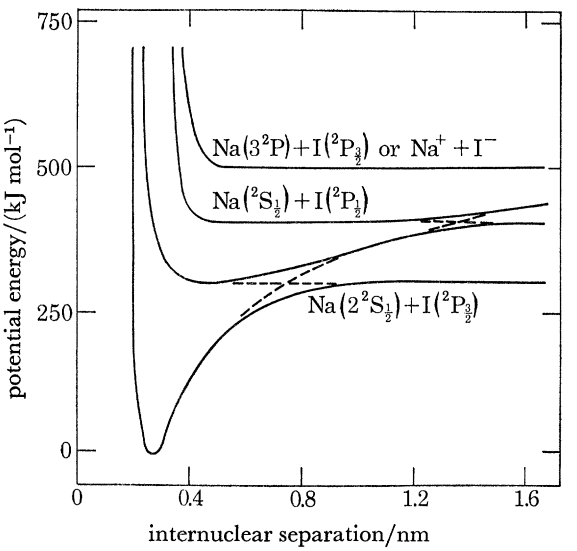

Figure 12. The potential energy curves for Na and I with both atoms in their ground states and each one in turn in their first electronically excited level. The energy for excited Na with ground state I is very close to that of Na^+ and I^- at infinite separation.

interaction between atoms is a weak van der Waals one and figure 12 has been drawn with only repulsive forces between them. This contrasts with Na^+ and I^- experiencing strong Coulombic forces. If the Born–Oppenheimer approximation is valid, the non-crossing rule predicts that ionic and covalent potential energy curves do not cross when they have the same symmetry. This is shown in figure 12. In fact, the adiabatic non-crossing rule breaks down, because the curves intersect at large internuclear separations, when the Born–Oppenheimer approximation does not hold completely. In this case the production of ions in process (II) involves atoms A and X approaching each other along a covalent curve and possibly changing over to the ionic state at a 'pseudocrossing'. Afterwards, the nuclei come together and then recoil, so that again there is the opportunity of a crossover, leading possibly to the production of ions after every

intersection has been traversed. Process (III) on the other hand must be seen as the collisional excitation of a molecule of AX from near the minimum of its ground state to upper vibrational levels. Dissociation of AX can then occur by a 'bleed-off' of particles from this vibrational distribution, to give either ions or atoms, depending on the exit channel. According to our measurements, k_3 is very small for certain molecules, such as LiBr, LiI, NaBr, NaI and all the halides of Ga and In. In these cases a dissociating molecule is unlikely to cross from the lower covalent potential energy curves to that leading to ions. Such crossovers evidently occur, however, for the other metal halides.

Figure 12 can be simplified for Cs and I in that $Cs(^2S_{\frac{1}{2}}) + I(^2P_{\frac{1}{2}})$ is higher in energy than $Cs^+ + I^-$ and so can be ignored. In some cases (Li with Br and I, Ga and In with I, and Tl with all three X) the $A(3\,^2P) + X(^2P_{\frac{3}{2}})$ is also lower in energy than $A^+ + X^-$ and results in another 'pseudocrossing'. Yet a further one has to be considered for Tl with Cl and Br, where $A\,(3\,^2P) + X\,(^2P_{\frac{1}{2}})$ 'intersects' the ionic state. The crossing distances ($R = R_c$) of any two potential energy curves can be calculated from $R_c = e^2/\Delta E$, where ΔE is the difference in energy between the two states at infinite internuclear separation and e is the electronic charge. The probability of a crossover from a covalent to an ionic state is described in terms of $H_{12}(R_c)$, the coupling matrix element of the Hamiltonian, evaluated at the crossing point. This corresponds to one half of the energy separation between the curves at the avoided crossing. The estimation of $H_{12}\,(R_c)$ has been carried out extensively (Magee 1952; Bates & Lewis 1955; Bates & Boyd 1956; Smirnov 1965; Van den Bos 1970; Olson *et al.* 1971; Grice & Herschbach 1974; Hubers *et al.* 1976), as well as determined experimentally (Moutinho *et al.* 1971; Fluendy *et al.* 1970). The most recent parametrization of Hubers *et al.* (1976) generally gives $H_{12}(R_c)$ midway between the others, but not very different from them, and so has been used here. The probability ρ of an electron jump occurring at a crossing point is usually calculated from Landau–Zener theory (Landau 1932; Zener 1932), which gives

$$\rho = \exp\left\{\frac{-2\pi[H_{12}(R_c)]^2}{\hbar v\, \mathrm{d}|V_1 - V_2|_{R_c}/\mathrm{d}R}\right\},$$

where v is the relative velocity of the nuclei, and V_1 and V_2 are the potentials of the two diabatic curves. Putting $V_1 = \Delta E - e^2/R_c$ and $V_2 = 0$ gives

$$\rho = \exp\left\{\frac{-2\pi R_c^2[H_{12}(R_c)]^2}{e^2\hbar v}\right\}. \tag{11}$$

If only one 'pseudocrossing' has to be considered then the probability of ions recombining in the reverse of (II) is then $2\rho\,(1-\rho)$ per collision.

8.2. *Reaction (II) and the computation of k_{-2}*

The cross section σ for ion–ion recombination in (II) is an impact-parameter averaged probability, which depends on the approach velocity and nature of the interaction between colliding ions. In fact (Bates & Boyd 1956; Baede 1975), by reference to equation (11) it is given by

$$\sigma = 4\pi P_R R_c(1 + \Delta E/E)\, F(\eta),$$

where

$$\eta = \frac{4\pi^2 e^2 \mu^{\frac{1}{2}}[H_{12}(R_c)]^2}{2^{\frac{1}{2}}\hbar(E+\Delta E)^{\frac{1}{2}}(\Delta E)^2}.$$

Here the reduced mass of the colliding ions is μ, E their initial energy and P_R is the probability of the systems making their approach along the appropriate potential curve. For ground state

atoms $A(^2S_{\frac{1}{2}}) + X(^2P_{\frac{3}{2}})$, eight molecular states emerge, only one of which is of the same symmetry as $A^+(^1S_0) + X^-(^1S_0)$, yielding $P_R = \frac{1}{8}$. For the crossing with $A(^2S_{\frac{1}{2}}) + X(^2P_{\frac{1}{2}})$, $P_R = \frac{1}{4}$. To derive the recombination coefficient, k_{-2}, the cross section is multiplied by the relative velocity and averaged over a Maxwell–Boltzmann distribution, which results (Bates & Boyd 1956) in

$$k_{-2} = \frac{0.51 P_R}{\mu^{\frac{1}{2}} (\Delta E)^2 T^{\frac{3}{2}}} F'(\beta), \tag{12}$$

where

$$\beta = 247 \mu^{\frac{1}{2}} [H_{12}(R_c)^2] / (\Delta E)^2.$$

With the tabulations of Bates & Boyd (1956) for $F'(\beta)$, it is relatively simple to calculate k_{-2}, once $H_{12}(R_c)$ is known. This has been done for the products of recombination being exclusively either A + X in their ground states or with X wholly in its first excited electronic state, but considering only one 'pseudocrossing' in each case. The results are given in table 5 for a temperature of 2000 K. Of course, in a real situation atoms of X will probably be produced in at least both states, so that the relevant overall k_{-2} could well be compounded from the two in table 5. A comparison of these computed k_{-2} is facilitated by plotting them logarithmically against ΔE as the circles in figure 13. It is seen there that the two sets of theoretical points cluster around smooth curves, with that for the products in their ground states being the lower. This smooth dependence on ΔE is to be expected, since β and $H_{12}(R_c)$ are both well behaved functions of ΔE. Each theoretical rate constant is seen to first increase sharply with ΔE, pass through a maximum and then decay. This can be explained by the probability of recombination being dependent on $2\rho\ (1-\rho)$. Clearly for large and small ρ, little overall recombination occurs, because reaction is most likely at $\rho = \frac{1}{2}$, corresponding to $\Delta E \sim 180\,\mathrm{kJ\,mol^{-1}}$. A further feature of figure 13 is that recombination to the ground states of A and X occurs at higher ΔE and consequently at a smaller crossing distance R_c, than for the production of excited halogen atoms. Because $2\rho(1-\rho)$ shows a maximum in ΔE and also on account of the higher P_R, the computed recombination coefficient may well be greater for the production of excited atoms of X than ground state ones. This is certainly the case for the group III b metals and possibly Li, too, i.e those atoms of highest ionization potential. In fact, for Tl and I the discrepancy is as large as a factor of 70. Generally speaking, the opposite is true for the remaining alkali metals, typified by K and Cl, or Na and I, where recombination to ground state products is computed to be at least 16 times more likely than to Cl in its first excited state. Of course, the principle of microscopic reversibility would indicate that the reverse ionization process: $A + X \longrightarrow A^+ + X^-$ originates primarily from excited X for the III b metals, and entirely from ground state X with most alkali metals, but with some combinations of A and X being intermediate.

We can now compare the experimentally observed k_{-2} with these theoretical predictions and will do so first for the group III b metals. Both table 5 and figure 13 indicate that k_{-2} was measured directly and unambiguously only with Ga and In, where recombination in the backward step of (III) is relatively unimportant and does not complicate the situation. These k_{-2} observed for Ga and In are large and in fact greater than the computed k_{-2} leading to electronically excited X, but only by a factor varying from 1.4 to 4.4. Agreement between experiment and Landau–Zener theory to this extent is just within their combined bounds of error and does establish for these group III b metals that the products of recombination are ground state A and electronically excited X. Examination of the k_{-2} obtained from the experimental k_2 and statistical mechanical K_2 (see table 5) shows that for Ga and In these are less than the k_{-2} measured directly by up to

as much as 65. Also, these indirectly observed k_{-2} are within a factor of 2 equal to those computed for recombination to ground state A and X. This indicates that ionization in the forward step of (II) involves only ground state atoms, a conclusion which is corroborated by the observation made above that the activation energy for ionization is the endothermicity for reactants in their ground states. For the group III b metals we thus have the interesting situation that k_2 does not equal $k_{-2}K_2$, which is a breakdown of the principle of detailed balancing, and arises from different states of X participating in ionization and recombination. This discrepancy between the two measured k_{-2} is seen from table 5 to be largest with Br and I, where the difference in energy

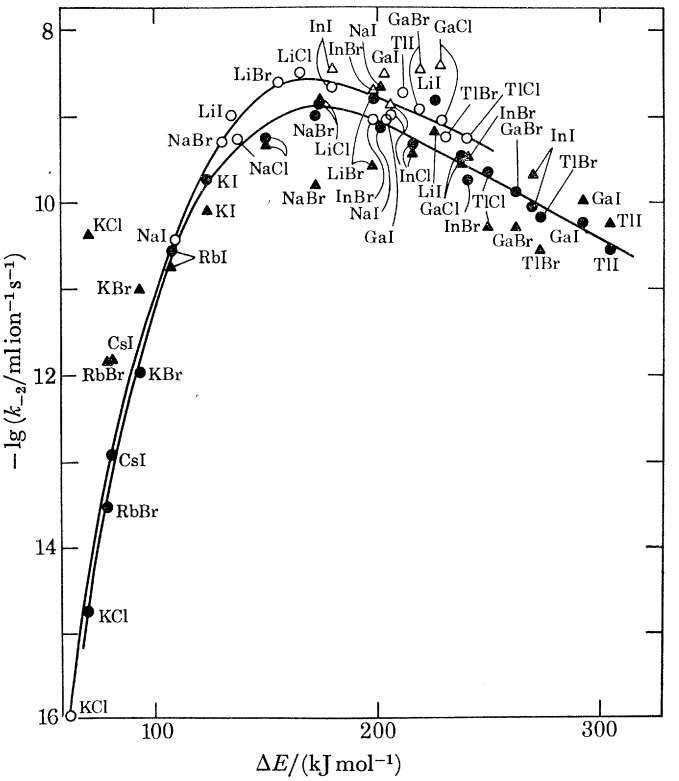

FIGURE 13. Values of $\lg k_{-2}$ plotted against ΔE for reaction (II). ▲, values from the experimental value of k_2 and the computed K_2: they are plotted as if only ground state atoms of A and X are involved; △, those measured directly for Ga and In, with ΔE that for the halogen atom in its first excited state; ●, computed magnitudes for ground state products; ○, computed values for ground state A and electronically excited X.

between the $^2P_{\frac{3}{2}}$ and $^2P_{\frac{1}{2}}$ states is 44 and 91 kJ mol^{-1}, respectively. These values are much greater than the figure of 10.5 kJ mol^{-1} for Cl. Even so, the conclusion that electronically excited X (called below X*) do not participate in ionization is somewhat surprising in that low excited states of metal atoms are rapidly populated in flames and quite often to an extent greater than that for equilibrium (Padley & Sugden 1958, 1959). Furthermore, collisional ionization in (I) has been thought (Hollander *et al.* 1963; Jensen & Padley 1966*b*; Kelly & Padley 1972) to depend on the electronic states of A being thermally populated up to the ionization threshold, with the rate-determining step being the loss of an electron from a highly excited A. The lack of detailed balancing in reaction (II) cannot be associated with the way potential energy curves cross. This is because the ratio of the rate of ion production from ground state A and X to that from A + X* actually equals the ratio of ion-recombination rates to these ground and first excited

states, as required by microscopic reversibility. In fact, both ratios can be shown to be proportional to $\rho_1(1-\rho_1)/\{(1-\rho_2)(\rho_1^2-\rho_1+1)\}$, where ρ_1 and ρ_2 are the crossover probabilities at the 'pseudocrossings' of the lowest and first excited covalent potential energy curves with the ionic one, respectively. Furthermore, it is improbable that there is little ionization from X* since $[X^*] \ll [X]$ at equilibrium. This is because the lower $[X^*]$ are offset by the activation energy for $A + X^* \longrightarrow A^+ + X^-$ being less than that for ionization from $A + X$ by the energy for $X \longrightarrow X^*$, as shown by figure 12. The most probable explanation seems to be that electronic excitation of X to X* is too slow for X* to play any significant rôle producing ions in the forward step of (II). The converse of this is that during ion recombination predominantly to X*, we might expect a population inversion; this is discussed below. However, there is evidence for electronic excitation in $X \longrightarrow X^*$ being slow from measurements of quenching cross sections of excited atoms. They (Donovan & Husain 1966; Jenkins 1968) indicate that $X + N_2 \longrightarrow X^* + N_2$ is slower by factors of 2×10^4 for Br and 10^5 for I than is $A + N_2 \longrightarrow A^* + N_2$, which occurs every collision. Excitation to X* by H_2 and H_2O, the other major constituents of the burnt gases of a flame (Deakin & Husain 1972), is somewhat more efficient than with N_2, but overall, the process appears slow enough to ensure that ionization in the forward step of (II) originates from ground state $A + X$. This state of affairs is likely to hold irrespective of the nature of A. In conclusion, it should be stressed that the k_{-2} in the third column of table 5 (i.e. those derived from k_2/K_2) for Ga, In and Tl are not the correct ones, the best estimates being those measured directly and given in the fourth column. If one were to recommend values of k_{-2} for $Tl^+ + X^-$, all three would be the same at $3 \pm 2 \times 10^{-9}$ ml ion^{-1} s^{-1}, in view of the independence of the computed and measured k_{-2} for Ga and In on the nature of A and X.

Unfortunately, this work did not produce direct measurements of k_{-2} for the alkali metals, so that no test of the relationship $K_2 = k_2/k_{-2}$ can be made. Looking first at both sets of computed k_{-2} for the alkali metals in table 5, it is clear that there is a gradation from Li, where the two k_{-2} are similar, to Rb and Cs, which have exceedingly small values ($< 10^{-20}$ ml ion^{-1} s^{-1}) when X is excited. The indirectly measured k_{-2} compare fairly well with Hayhurst & Sugden's (1967) previously determined values, using the less accurate approach depending on $[A^+]$ being close to its steady state level. Otherwise, these experimental k_{-2} agree with the theoretical ones to within a factor of 3 for Cl with Li and Na, where the two computed k_{-2} are very similar, and I with Li, K and Rb. The worst agreement is with K + Cl, Rb + Br, K + Br and Cs + I, which are higher than the largest theoretical values by factors of 2×10^4, 50, 10 and 10, respectively. These cases will be discussed again below. Broadly speaking, though, the plot of these experimental k_{-2} in figure 13 does show that, apart from these few exceptions, they are following the predictions of Landau–Zener theory. There is no experimental evidence to suggest that ionization cannot take place from excited, as well as ground state X, but of course for Br and I effectively every free atom will be in its ground state, because of the large excitation energy and the relative slowness of electronic excitation. The theoretical computations of k_{-2} on the other hand are unequivocal for K, Rb and Cs, where only ground state $A + X$ can participate in process (II). For these metals we would expect the relationship $K_2 = k_2/k_{-2}$ to be true and the experimental k_{-2} in the third column of table 5 to be realistic. As for Li and Na, detailed balancing might not always strictly hold, but this is not likely to lead to large errors in the experimentally derived k_{-2}, except possibly for Li with Br and I, which might be too low by a factor of around 2. Broadly speaking, then, each direction of process (II) for the alkali metals involves almost exclusively ground state $A + X$, in contrast to Ga, In and Tl.

A complication of this situation could arise in that at high crossing distances, the Landau–Zener model may not exactly represent an electronic transition, whenever the two colliding species spend a significant proportion of their collision time with some covalent and the ionic state approximately degenerate. This can lead to a transition from one state to another (i.e. electron transfer) well away from the crossing of such potential energy curves. This has been shown (Weiner *et al.* 1971) to be the case for $Na^+ + O^- \longrightarrow O(^3P) + Na(3d)$, which is nearly thermoneutral and gives a crossing at 28.8 nm. Landau–Zener theory, which only considers transitions at a 'pseudocrossing' leads to an extremely small cross section for this process and the experimental value of $4 \times 10^{-17}\,m^2$ suggests a breakdown of that model. In addition, the endothermic reaction (by $13.5\,kJ\,mol^{-1}$): $Na^+ + O^- \longrightarrow O(^2P) + Na(4p)$ was found to have a cross section of $\sim 10^{-18}\,m^2$, which is also incompatible with curve-crossing theory. However, recombination to Na(3p) in this system by a crossing at around 1 nm apparently has a smaller cross section, more in line with Landau–Zener theory. Thus the possibility of electron transfer at large internuclear separations can lead to both recombination and ionization rates being enhanced above the expectations of simple curve-crossing theory. This is most probably the explanation of the few anomalously large observed k_{-2} depicted in figure 13. For instance, Olson (1977) has computed k_{-2} for the recombination of $K^+ + Cl^-$ using both Landau–Zener and close-coupling techniques. The latter allow transitions over a wide range of distances on either side of a curve crossing, provided the potential energy curves lie close together. His computed Landau–Zener cross sections are 'several orders of magnitude below the close-coupling' ones, which in fact is in line with our observed k_{-2} for $K^+ + Cl^-$ being not only some 2×10^4 times larger than Landau–Zener theory predicts, but also within a factor of 2 equal to that from Olson's close-coupling computations. We have already noted in figure 12 a near-degeneracy between excited Na with ground state I atoms and the pair $Na^+ + I^-$. Since there is relatively rapid electronic excitation of metal atoms in flames (Padley & Sugden 1958), we might expect the participation of such states occasionally to enhance overall ionization and recombination rates. In fact, table 5 indicates that the measured k_{-2} exceeds that predicted by curve-crossing theory by a factor of 3.2 for Na and I. Similar explanations are available for the other anomalously large observed k_{-2} noted above. They are substantiated by Gait & Berry's (1977) recent observation that population inversions can be produced in the 3p state of Na atoms during ion recombination in $Na^+ + I^- \longrightarrow Na\,(3p) + I(^2P_{\frac{1}{2}})$, which is almost thermoneutral, as seen above. Population inversions have also been observed (Berry *et al.* 1968; Mandl 1971; Luther *et al.* 1972) for negative ions, when a salt like CsBr dissociates primarily to ions on being heated in a shock tube. No one, so far, appears to have observed the population inversion in excited halogen atoms, expected from our observations of ions recombining in $A^+ + X^- \longrightarrow A + X^*$ for A being Ga, In or Tl.

8.3. *Reaction* (III) *and the computation of* k_{-3}

As indicated above, the dissociation of AX occurs from some distribution dissociation limit. These species can dissociate either by an adiabatic channel to produce atoms or by a diabatic one, with curve crossing to yield ions. Several experimental studies have been made of this dissociation in shock tubes, as well as there being theoretical work (Berry *et al.* 1968; Hartig *et al.* 1968; Mandl 1971; Ewing *et al.* 1971; Luther *et al.* 1972; Milstein 1973). By monitoring the species formed in an incident shock, it proved possible to determine the fraction of the halide dissociating into atoms or ions, and also to correlate this with theoretical predictions. Ewing *et al.* (1971)

based their correlation on the adiabatic channel width (E_{AD}), i.e. that impact energy at which the probability of diabatic behaviour is 1/e. They were able to show that this quantity depended strongly on R_c and $H_{12}(R_c)$, and found that for large E_{AD} dissociation proceeds to atoms, for small values to ions, and for intermediate values, a mixture of atoms and ions is produced. They found good qualitative agreement between their observations and these theoretical predictions, with NaBr, NaI, LiBr and LiI dissociating completely to atoms, LiCl, NaCl and KI producing mixtures and the remainder dissociating totally to ions. We have carried out similar calculations for the group III b halides and they indicate that only atoms should be produced. This work with flames agrees very well with all these results, in so far as table 3 shows $k_3 \sim 0$ for NaBr, NaI, LiBr, LiI and all the halides of Ga and In, corresponding to dissociation to atoms.

TABLE 6. VALUES OF k_{-3} (IN UNITS 10^{-28} ml particle^{-1} s^{-1}) CALCULATED FROM BATES & FLANNERY'S THEORY AT 2000 K FOR M = H_2, H_2O AND N_2, AND A COMPARISON OF THEIR AVERAGE WITH THAT OBSERVED

A	X	$k(H_2)$	$k(H_2O)$	$k(N_2)$	k_{av}	exp k_{-3} (2000 K)
Li	Cl	5.1	6.9	7.3	6.9	17
Li	Br	5.3	6.3	6.3	6.1	$<4.4\,(-4)$
Li	I	5.5	6.3	5.9	5.9	$<2.0\,(-4)$
Na	Cl	2.3	5.1	5.9	5.2	11
Na	Br	1.9	4.3	4.3	4.0	$<1.2\,(-3)$
Na	I	2.1	4.1	4.4	4.0	$<5.6\,(-3)$
K	Cl	1.7	4.3	5.1	4.4	14
K	Br	1.1	3.1	3.7	3.2	12
K	I	1.2	2.9	3.5	3.1	15
Rb	Cl	1.0	3.3	3.9	3.4	8.8
Rb	Br	0.82	2.1	2.7	2.3	11
Rb	I	0.66	1.7	2.2	2.0	7.7
Cs	Cl	0.67	3.3	3.6	3.1	5.8
Cs	Br	0.41	1.8	2.6	2.1	5.1
Cs	I	0.089	1.1	1.6	1.2	2.6
Tl	Cl	0.57	3.0	3.5	2.9	2.6
Tl	Br	0.39	1.9	2.2	1.9	2.6
Tl	I	0.23	0.91	1.4	1.1	2.1

The exception is that of the Tl halides, for which $k_3 \neq 0$. This is probably due to dissociation occurring partly along exit channels with excited Tl (^{2}P) atoms, as noted above, with crossovers at high inter-particle separations favouring ionic dissociation.

This shock tube work has been extended by Mandl (1971), Luther *et al.* (1972) and Milstein (1973), who have determined k_3 with Ar as the third body and assuming that $k_3 = A_3\,T^{-3.5} \exp(-\Delta E_3/RT)$. A crucial difference between the results from this shock tube work and that presented above is that the measured activation energies are much less than the endothermicity, ΔH_3 (in fact, they find that typically $\Delta E_3 \sim 0.4\,\Delta H_3$), whereas we conclude $\Delta E_3 = \Delta H_3$. With these discrepancies it is difficult to compare our rate constants with those of these workers, although fair agreement holds between the various set of k_3 at around 2700–3000 K. It seems that dissociation in a shock front might have a 'bottleneck' in the equilibration of the upper vibrational levels, with possibly depopulation of these states occurring in the time available, of up to 40 μs.

The dissociation rate constants k_3 can be considered in terms of its reverse recombination coefficient k_{-3} using the theory of Bates & Flannery (1968). This assumes a rapid establishment

of a quasi-equilibrium of ion pairs, which are slowly deactivated by a third body. The rate constant turns out to be $k_{-3} = 1.3 \times 10^{-8} e\alpha^{\frac{1}{2}} nG(m_1, m_2, m_3, S_{12}, S_{13}, T, \alpha)$, where α is the polarizability of M, n the concentration of particles and G is a tabulated function of the masses m_1, m_2, m_3 and colliding particle radii S_{12}, S_{13}, for species 1, 2 and 3. The k_{-3} measured above in flames refer to the sum of three individual contributions from collisions with H_2, N_2 and H_2O. Table 6 gives these three computed recombination coefficients, together with their net value, averaged for a flame at 2000 K, in which $[H_2] : [H_2O] : [N_2] = 0.139 : 0.255 : 0.606$. In addition, table 6 compares these with the experimental values, derived as $k_3 K_3^{-1}$ in flame 4 at close to 2000 K. It is seen that, if we forget the very small values governed by curve-crossing considerations, the experimental k_{-3} are around 3 times larger than the theoretical ones, the largest discrepancy being by a factor of 4.8. This is not bad agreement, considering the errors of each quantity. In addition, there is no evidence from table 6 to suggest that detailed balancing does not hold for reaction (III), which means that the values of A_{-3} in table 3 can be used with confidence to predict k_{-3}.

Bates & Flannery's theory of ion recombination does not take curve-crossing into consideration. This is normally justified by reverting to Thomson's theory (1924) and the concept of a critical radius, within which the probability of an ion pair being deactivated is close to unity. This critical collision diameter can be calculated as $3e^2/2kT$, or about 6 nm at 2000 K. Since all the crossover distances are less than this, collisional deactivation can usually occur without any necessity for crossover.

This work was financed by the Science Research Council. We are most grateful for this, as well as to Dr D. E. Jensen for several helpful conversations.

References

Ashton, A. F. & Hayhurst, A. N. 1973 *Combust. Flame*, **21**, 69.
Baede, A. 1975 *Adv. Chem. Phys.* **30**, 463.
Barrett, A. H. & Mandel, M. 1958 *Phys. Rev.* **109**, 1572.
Bates, D. R. & Boyd, T. J. M. 1956 *Proc. Phys. Soc.* A **69**, 910.
Bates, D. R. & Flannery, M. R. 1968 *Proc. R. Soc. Lond.* A **302**, 367.
Bates, D. R. & Lewis, J. T. 1955 *Proc. Phys. Soc.* A **68**, 173.
Berry, R. S., Cernoch, T., Coplan, M. & Ewing, J. J. 1968 *J. Chem. Phys.* **49**, 127.
Bulewicz, E. M., Phillips, L. F. & Sugden, T. M. 1961 *Trans. Faraday Soc.* **57**, 921.
Bulewicz, E. M. & Sugden, T. M. 1958 *Trans. Faraday Soc.* **54**, 830.
Burdett, N. A. & Hayhurst, A. N. 1976 *J. Chem. Soc. Faraday Trans.* (I) **72**, 245.
Burdett, N. A. & Hayhurst, A. N. 1977*a* *Proc. R. Soc. Lond.* A **355**, 377.
Burdett, N. A. & Hayhurst, A. N. 1977*b* *Chem. Phys. Lett.* **48**, 95.
Burdett, N. A. & Hayhurst, A. N. 1978 *J. Chem. Soc. Faraday Trans.* (I) **74**, 63.
Deakin, J. J. & Husain, D. 1972 *J. Chem. Soc. Faraday Trans.* (I) **68**, 41.
Donovan, R. J. & Husain, D. 1966 *Trans. Faraday Soc.* **62**, 2987.
Ewing, J. J., Milstein, R. & Berry, R. S. 1971 *J. Chem. Phys.* **54**, 1752.
Fluendy, M. A. D., Horne, D. S., Lawley, K. P. & Morris, A. W. 1970 *Mol. Phys.* **19**, 659.
Gait, P. D. & Berry, R. S. 1977 *J. Chem. Phys.* **66**, 2387, 2764.
Gaydon, A. G. & Wolfhard, H. G. 1970 *Flames, their structure, radiation and temperature* (3rd edn). London: Chapman and Hall.
Gordy, W. & Cook, R. L. 1970 *Microwave molecular spectra, part II, Chemical applications of spectroscopy* (2nd edn) (ed. W. West). New York: Wiley–Interscience.
Green, J. A. & Sugden, T. M. 1963 *9th International symposium on combustion*, p. 607. New York: Academic Press.
Grice, R. & Herschbach, D. R. 1974 *Mol. Phys.* **27**, 159.
Hartig, R., Olschewski, H. A., Troe, J. & Wagner, H. G. 1968 *Ber. Bunsengesellschaft* **72**, 1016.
Hayhurst, A. N. & Kittelson, D. B. 1974 *Proc. R. Soc. Lond.* A **338**, 155.
Hayhurst, A. N. & Kittelson, D. B. 1977 *Combust. Flame* **28**, 137.

Hayhurst, A. N. & Kittelson, D. B. 1978 *Combust. Flame* **31**, 37.
Hayhurst, A. N., Mitchell, F. R. G. & Telford, N. R. 1971 *Int. J. Mass Spec. Ion. Phys.* **7**, 177.
Hayhurst, A. N. & Sugden, T. M. 1963 *Inst. El. Eng. Conf. Rep. Ser.* **4**, 126.
Hayhurst, A. N. & Sugden, T. M. 1967 *Trans. Faraday Soc.* **63**, 1375.
Hayhurst, A. N. & Telford, N. R. 1970 *Trans. Faraday Soc.* **66**, 2784.
Hayhurst, A. N. & Telford, N. R. 1972 *J. Chem. Soc. Faraday Trans.* (I) **68**, 237.
Hayhurst, A. N. & Telford, N. R. 1977 *Combust. Flame* **28**, 67.
Hershey, H. C., Zakin, J. L. & Simha, R. 1967 *Ind. Eng. Chem.* (*Fund*) **6**, 413.
Herzberg, G. 1960 *Spectra of diatomic molecules*. Princeton: Van Nostrand.
Herzberg, G. 1966 *Electronic structure and electronic spectra of polyatomic molecules*. Princeton: Van Nostrand.
Hollander, T., Kalff, P. J. & Alkemade, C. T. J. 1963 *J. chem. Phys.* **39**, 2558.
Honig, A., Madel, M., Stitch, M. L. & Townes, C. H. 1954 *Phys. Rev.* **96**, 629.
Hubers, M. M., Kleyn, A. W. & Los, J. 1976 *Chem. Phys.* **17**, 303.
James, C. G. & Sugden, T. M. 1955 *Proc. R. Soc. Lond.* A **227**, 312.
J.A.N.A.F. Thermochemical Tables 1965 Michigan: Dow Chemical Company.
Jenkins, D. R. 1968 *Proc. R. Soc. Lond.* A **303**, 453, 467; A **306**, 413.
Jenkins, D. R. & Sugden, T. M. 1969 *Flame emission and atomic absorption spectrometry*, vol. 1, p. 151. New York and London: Marcel Dekker.
Jensen, D. E. & Jones, G. A. 1974 *J. Chem. Phys.* **60**, 3421.
Jensen, D. E. & Padley, P. J. 1966*a* *Trans. Faraday Soc.* **62**, 1.
Jensen, D. E. & Padley, P. J. 1966*b* *Trans. Faraday Soc.* **62**, 2140.
Jensen, D. E. & Pergament, H. S. 1971 *Combust. Flame* **17**, 115.
Kelly, R. & Padley, P. J. 1969 *Trans. Faraday Soc.* **65**, 355.
Kelly, R. & Padley, P. J. 1971 *Trans. Faraday Soc.* **67**, 740.
Kelly, R. & Padley, P. J. 1972 *Proc. R. Soc. Lond.* A **327**, 345.
Klemperer, W. & Rice, S. A. 1957 *J. Chem. Phys.* **26**, 618.
Knewstubb, P. F. & Sugden, T. M. 1959 *7th International symposium on combustion*, p. 247. London: Butterworths.
Landau, L. D. 1932 *Phys. Z. Sowjetunion* **2**, 46.
Luther, von K., Troe, J. & Wagner, H. G. 1972 *Ber. Bunsengesellschaft* **76**, 53.
Mandl, A. 1971 *J. Chem. Phys.* **55**, 2918, 2922.
Magee, J. L. 1952 *J. Chem. Phys.* **8**, 687.
Milstein, R. 1973 Ph.D. Dissertation, University of Chicago.
Moutinho, A. M. C., Aten, J. A. & Los, J. 1971 *Physica* **53**, 471.
Olson, R. E. 1977 *Combust Flame* **30**, 243.
Olson, R. E., Smith, F. T. & Bauer, E. 1971 *Appl. Optics* **10**, 1848.
Padley, P. J., Page, F. M. & Sugden, T. M. 1961 *Trans. Faraday Soc.* **57**, 1552.
Padley, P. J. & Sugden, T. M. 1958 *Proc. R. Soc. Lond.* A **248**, 248.
Padley, P. J. & Sugden, T. M. 1959 *7th International symposium on combustion*, p. 235. London: Butterworths.
Phillips, L. F. & Sugden, T. M. 1960 *Can. J. Chem.* **38**, 1804.
Rice, S. A. & Klemperer, W. 1957 *J. Chem. Phys.* **27**, 573.
Smirnov, B. M. 1965 *Soviet Phys. Dokl.* **10**, 218.
Thomson, J. J. 1924 *Phil. Mag.* **47**, 337.
Van den Bos, J. 1970 *J. Chem. Phys.* **52**, 3254.
Weiner, J., Peatman, W. & Berry, R. S. 1971 *Phys. Rev.* A **4**, 1824.
Zener, C. 1932 *Proc. R. Soc. Lond.* A **137**, 696.

PHILOSOPHICAL TRANSACTIONS OF THE ROYAL SOCIETY A MATHEMATICAL, PHYSICAL & ENGINEERING SCIENCES